



incoming phonological information (Hickok & Poeppel, 2004, 2007). This view is supported by studies that implicate AF signals for reactivating phonological material in verbal working memory (Friedmann & Gvion, 2003) and short-term storage and verbal repetition of speech (Glasser & Rilling, 2008; Rilling et al., 2008; Saur et al., 2008; Catani & Ffytche, 2005). These theoretical models of AF function are based on behavioral deficits in conduction aphasics and the functional role of the cortical regions connected by the arcuate. However, there is very little research on the relationship between variance in AF anatomy in healthy subjects and variance of the particular skills that are hypothesized to depend on the signals carried by AF axons.

Beyond models of language processing, models of reading have recently featured the AF. Whole-brain voxel-based group analysis of white matter diffusion properties found a group difference between adult good and poor readers and a correlation between white matter microstructure and reading skills, located in the vicinity of the AF (Supplementary Figure 1; Klingberg et al., 2000). The existence of a microstructural white matter difference between good and poor readers has been independently replicated in children by several laboratories (Niogi & McCandliss, 2006; Beaulieu et al., 2005; Deutsch et al., 2005). Although the reading-related differences are located medial to the AF and not in the AF itself, the findings may still be interpreted as stemming from interdigitating, medial AF fibers (Ben-Shachar et al., 2007; Beaulieu et al., 2005). If this is true, it is possible that the AF contributes to reading based on its role in phonological processing, because phonological skills are an essential factor in reading development (Wagner & Torgesen, 1987).

Most of these studies applied whole-brain voxel-based methods, searching for group differences and correlations between DTI measures and reading skill. Whole-brain methods are valuable in the absence of a specific hypothesis, but they lack anatomical specificity, because the same voxel in a normalized brain may map to different tracts across individuals. A further limitation of whole-brain methods is reduced statistical power because of the large number of statistical comparisons. Hence, whole-brain methods are not optimal for testing specific anatomical hypotheses.

Here, we capitalize on recent advances in fiber tracking methods to identify the AF as an ROI in individual subjects. We then test the specific hypothesis that the diffusion measures within this tract covary with standardized measures of phonological memory, phonological awareness, and reading skills. We further explore how laterality of the tract relates to behavior and how the subject's sex modulates these effects to follow up on recent reports (Lebel & Beaulieu, 2009; Catani et al., 2007; Lenroot et al., 2007). Our results provide empirical support for the hypothesis that the AF is part of the reading circuitry and that maturation of the arcuate is important for the development of reading-related skills.

## METHODS

### Subjects

Fifty-five children aged 7–11 years participated in this study. The data analyzed here represent the first measurement in a longitudinal study of reading development. Participants were physically healthy and had no history of neurological disease, head injury, attention deficit/hyperactivity disorder, language disability, or psychiatric disorder. Screening for attention deficit/hyperactivity disorder was based on the child's history and on the Conners' Parent Rating Scale (Revised Short Form), which confirmed that all subjects scored in the normal range (<65). All participants were native English speakers and had normal or corrected-to-normal vision and normal hearing. The Stanford Panel on Human Subjects in Medical and Nonmedical Research approved all procedures. Written informed consent/assent was obtained from all parents and children.

### Behavioral Testing

Participants completed a 4-hr battery of cognitive tests to characterize their reading skills, phonological awareness, rapid naming, and general intelligence. Descriptive statistics on this sample have been previously reported (Dougherty et al., 2007). On the basis of our specific hypotheses regarding the AF's role in phonology and reading, we included the following three age-standardized behavioral measures in this study:

- (a) *Phonological Memory*: The phonological memory composite score measures an individual's ability to code information phonologically for temporary storage in working memory. This score is composed of two subtests: digit span and nonword repetition (Wagner, Torgesen, & Rashotte, 1999).
- (b) *Phonological Awareness*: The phonological awareness composite score measures an individual's ability to parse the word into syllables and phonemes and manipulate these phonemes to make up new words. The score is composed of two subtests that measure the ability to segment and blend phonemes (elision and blending; Wagner et al., 1999).
- (c) *Basic Reading*: The basic reading composite score assesses a child's accuracy at reading single words and pseudowords. It is composed of two subtests: word identification, which measures accuracy in reading aloud a list of words (untimed), and word attack, which measures accuracy in reading aloud a list of pseudowords (untimed; Woodcock, McGrew, & Mather, 2001).

### DTI

MRI data were acquired on a 1.5-T Signa LX scanner (Signa CVi; GE Medical Systems, Milwaukee, WI) using a self-shielded, high-performance gradient system. A standard

quadrature head coil, provided by the vendor, was used for excitation and signal reception. Head motion was minimized by placing cushions around the head and securing a strap across the forehead.

### Data Acquisition

The DTI protocol used eight repetitions of a 90-sec whole-brain scan. The scans were averaged to improve signal quality. The pulse sequence was a diffusion-weighted single-shot spin-echo EPI sequence (echo time [TE] = 63 msec; repetition time [TR] = 6 sec; field of view [FOV] = 260 mm; matrix size = 128 × 128; bandwidth = ±110 kHz; partial *k*-space acquisition). We acquired 60 axial, 2-mm-thick slices (no skip) for two *b* values, *b* = 0 and *b* = 800 sec/mm<sup>2</sup>. The high *b*-value data were obtained by applying gradients along 12 diffusion directions (six noncollinear directions). Two gradient axes were energized simultaneously to minimize TE, and the polarity of the effective diffusion-weighting gradients was reversed for odd repetitions to reduce cross-terms between diffusion gradients and imaging and background gradients. Although Jones (2004) suggests that measuring more diffusion directions might be more efficient at reliably estimating diffusion tensors of arbitrary orientation, our signal-to-noise ratio is sufficiently high from our eight repeats to produce very reliable tensor estimates. We have confirmed this in a subset of subjects by comparing bootstrapped tensor uncertainty estimates from 40 direction data with the 12 direction data reported here. With our high signal-to-noise ratio (SNR), tensor uncertainty is limited by physiological noise rather than measurement noise.

We also collected high-resolution T1-weighted anatomical images for each subject using an 8-min sagittal 3-D spoiled gradient recall (SPGR) sequence (voxel size = 1 × 1 × 1 mm). The following anatomical landmarks were defined manually in the T1 images: the anterior commissure (AC), the posterior commissure (PC), and the mid-sagittal plane. With these landmarks, we used a rigid body transform to convert the T1-weighted images to the conventional AC–PC aligned space.

### Data Preprocessing

Eddy current distortions and subject motion in the diffusion-weighted images were removed by a 14-parameter constrained nonlinear coregistration based on the expected pattern of eddy current distortions given the phase encode direction of the acquired data (Rohde, Barnett, Basser, Marengo, & Pierpaoli, 2004).

Each diffusion-weighted image was registered to the mean of the (motion-corrected) non-diffusion-weighted (*b* = 0) images using a two-stage coarse-to-fine approach that maximized the normalized mutual information. The mean of the non-diffusion-weighted images was automatically aligned to the T1 image using a rigid body mutual information algorithm. All raw images from the diffusion

sequence were resampled to 2-mm isotropic voxels by combining motion correction, eddy current correction, and anatomical alignment transforms into one omnibus transform and resampling the data using trilinear interpolation based on code from SPM5 (Friston & Ashburner, 2004).

An eddy current intensity correction (Rohde et al., 2004) was applied to the diffusion-weighted images at the resampling stage.

The rotation component of the omnibus coordinate transform was applied to the diffusion-weighting gradient directions to preserve their orientation with respect to the resampled diffusion images. The tensors were then fit using a robust least squares algorithm designed to remove outliers from the tensor estimation step (Chang, Jones, & Pierpaoli, 2005). We computed the eigenvalue decomposition of the diffusion tensor, and the resulting eigenvalues were used to compute for fractional anisotropy (FA; Basser & Pierpaoli, 1996). The FA is the normalized standard deviation of the three eigenvalues and indicates the degree to which the isodiffusion ellipsoid is anisotropic (i.e., one or two eigenvalues are larger than the mean of all three eigenvalues). The mean diffusivity is the mean of the three eigenvalues, which is equivalent to one third of the trace of the diffusion tensor.

We confirmed that the DTI and T1 images were aligned to within a few millimeters in the ROIs for this study. This confirmation was done by manual inspection by one of the authors (R.F.D.). In regions prone to susceptibility artifacts, such as orbito-frontal and inferior temporal regions, the misalignment was somewhat larger because of uncorrected EPI distortions.

All the custom image processing software is available as part of our open-source mrDiffusion package (revision 2289) available for download from [vistalab.stanford.edu/vistawiki/index.php/Software](http://vistalab.stanford.edu/vistawiki/index.php/Software).

### Fiber Tract Identification

To test the primary hypothesis, we manually identified the left AF for each individual. We developed three alternative methods to test the robustness and specificity of the results. First, we used an automated tract identification procedure to identify the arcuate. The main results were evaluated on the tracts identified by the manual and automated procedures. Second, we identified control tracts including the left superior longitudinal fasciculus (SLF), left corona radiata, and right AF to confirm the specificity of effects in the left AF. Third, we developed a tract alignment procedure to coregister anatomically equivalent portions of the left AF and reduce confounds caused by crossing fibers, tract curvature, and partial voluming with neighboring structures. These three procedures are described in detail in the Supplementary Material.

Figure 1 shows the three main steps of the manual AF segmentation procedure: tracking, restricting by a coarse ROI, and manual editing.

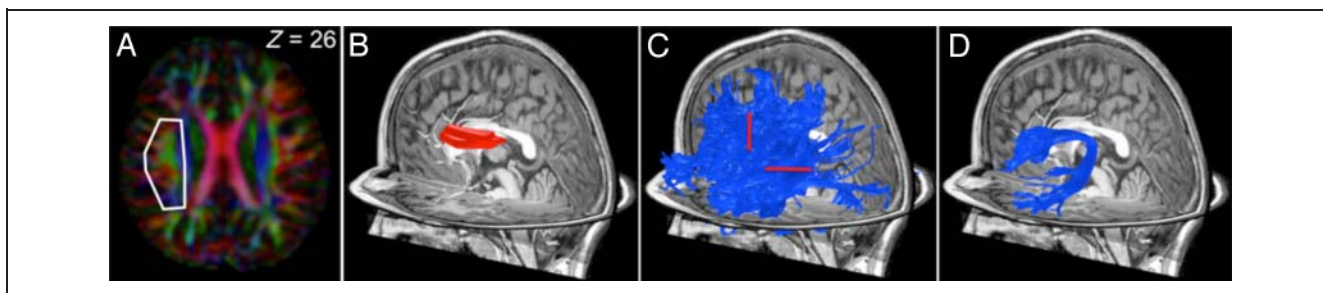


**Figure 1.** Method of identifying the AF in a single subject. Whole-brain streamlines tracing technique (STT) tractography produced a large collection of estimated tracks (not shown). An ROI in the white matter was drawn comprising the voxels with an anterior–posterior (green) PDD that are located adjacent and lateral to the cortical spinal tract. The cortical spinal tract can be identified because its PDD is in the inferior–superior (blue) direction. (A) The PDD at each voxel in a typical axial slice ( $Z = 26$ ). The white outline shows the region selected in this slice. The ROI is large so that all of the AF fibers will be included. (B) The complete ROI for this subject, which is selected from several adjacent planes. (C) Estimated fiber tracks passing through the ROI. We identify the AF fibers from the group by selecting the fibers that (1) project anterior to the central sulcus and (2) continue posterior and inferior into the temporal lobe (red lines). These waypoints were manually identified for each subject in an interactive fiber tract viewing and segmentation tool available for download at [vistolab.stanford.edu/software](http://vistolab.stanford.edu/software). (D) The estimated left AF for this subject.

**Tracking.** We manually identified the left AF in each individual based on a DTI atlas of human white matter (Mori, Wakana, van Zijl, & Nagae-Poetscher, 2005). We seeded the tracking algorithm with a mask of all left hemisphere voxels with an FA value of greater than 0.2 (Basser, Pajevic, Pierpaoli, Duda, & Aldroubi, 2000; Mori, Crain, Chacko, & van Zijl, 1999). Fiber tracts were estimated using a deterministic streamlines tracking algorithm (Basser et al., 2000; Mori et al., 1999) with a fourth-order Runge–Kutta path integration method and 1-mm fixed-step size. A continuous tensor field was estimated with trilinear interpolation of the tensor elements. Starting from initial seed points within the white matter mask, the path integration procedure traced streamlines in both directions along the principal diffusion axes. Individual streamline integration was terminated using two standard criteria: tracking is halted if (1) the FA estimated at the current position is below 0.15 or (2) the minimum angle between the last path segment and next step direction is  $>50^\circ$ .

**Restricting by a coarse ROI.** The ROI was defined based on red green blue (RGB) map that color codes the principal diffusion direction (PDD) within each voxel: red for left–right, green for anterior–posterior, and blue for superior–inferior. On each subject’s RGB map, we manually defined an ROI that encompassed all green voxels lateral to the internal capsule, between MNI plane  $z = 20$  and  $z = 30$  (Catani, Jones, & Ffytche, 2005; Figure 1A). This ROI was defined liberally, making sure to include all possible arcuate voxels and allowing voxels from neighboring tracts as well. The left hemisphere fiber group was limited to those fibers that intersected the ROI.

**Manual editing.** We manually selected fibers that (1) turned inferior at the temporal parietal junction and entered the temporal lobe and (2) continued anterior at the central sulcus and entered the frontal lobe (Figure 1C). We eliminated fibers that (1) headed ventrally toward the insula, (2) turned medially toward the corpus callo-

sum or medial frontal cortex, or (3) turned superiorly for the middle and superior frontal gyri. This procedure was implemented using a gesture-based interface (Akers, 2006). The procedure identified all the left hemisphere fibers that projected from the temporal lobe dorsally over the Sylvian fissure to the inferior frontal and precentral gyri, corresponding to the AF (Figure 1D).

**Calculating fiber tract summary measures.** We extracted the three tensor eigenvalues at each point along each fiber. From these, we calculated FA, mean diffusivity, radial diffusivity (RD), and axial diffusivity (AD) and averaged each measure along the entire tract. This method effectively computed a weighted-average because voxels with greater fiber density contributed more to the final measure than voxels with low fiber density. This weighting reduced the effects of partial voluming, because the fiber density is related to the likelihood that a voxel is filled with arcuate fibers.

We tested correlations between FA in the left arcuate and phonological memory, phonological awareness, and basic reading skills. For significant FA correlations, we examined RD (the mean of the second and third eigenvalues) and AD (the first eigenvalue) to determine which aspect of the diffusion characteristics best predicted behavior.

#### Arcuate Volume Estimation

We estimated the volume of the arcuate in two ways to ensure that significant findings reflect meaningful biological variation and are not dependent on our specific procedure. First, we obtained a volume estimate as a weighted sum of the number of voxels containing arcuate fibers. Each voxel’s contribution to the volume estimate was weighted by the ratio of arcuate fibers in the voxel compared with fibers from adjacent tracts in the voxel. This method reduces potential bias introduced by partial voluming with neighboring tracts, such as the frontal-parietal SLF. Second, we used the common method of simply

counting the estimated streamlines in each hemisphere's tract (Lebel & Beaulieu, 2009; Catani et al., 2007).

In some subjects, deterministic tractography fails to identify the right AF. This might imply that the right AF is absent (Lebel & Beaulieu, 2009; Catani et al., 2007), or alternatively, it might be explained by limitations of the deterministic algorithm in regions of crossing fibers (Wahl et al., 2010). For example, partial voluming between the right AF and branching SLF fibers could send deterministic tracking algorithms in the wrong direction. We used a new algorithm that combines probabilistic methods and quantitative predictions of the diffusion data to test the hypothesis that the right AF is missing (Sherbondy, Matthew, & Alexander, 2010; Sherbondy, Dougherty, Ananthanarayanan, Modha, & Wandell, 2009; Sherbondy, Dougherty, Ben-Shachar, Napel, & Wandell, 2008). The new method identifies the most likely candidate streamlines by evaluating the agreement between the pathway and the diffusion measurements. See Supplementary Method for more details.

## RESULTS

### The Left AF Tracts and Their Cortical Projection Zones

Figure 2 shows the distribution of AF cortical endpoints. For each subject, the endpoints were transformed into a common coordinate frame, and we calculated the number of subjects with fiber endpoints within 3 mm of each vertex on the cortical surface. Thus, the color overlay represents the likelihood, across subjects, of AF termination point at each cortical location.

The frontal lobe projection zone of AF fibers is fairly compact, falling mainly in the premotor cortex and Brodmann's area 44. The temporal lobe projection zone differs widely

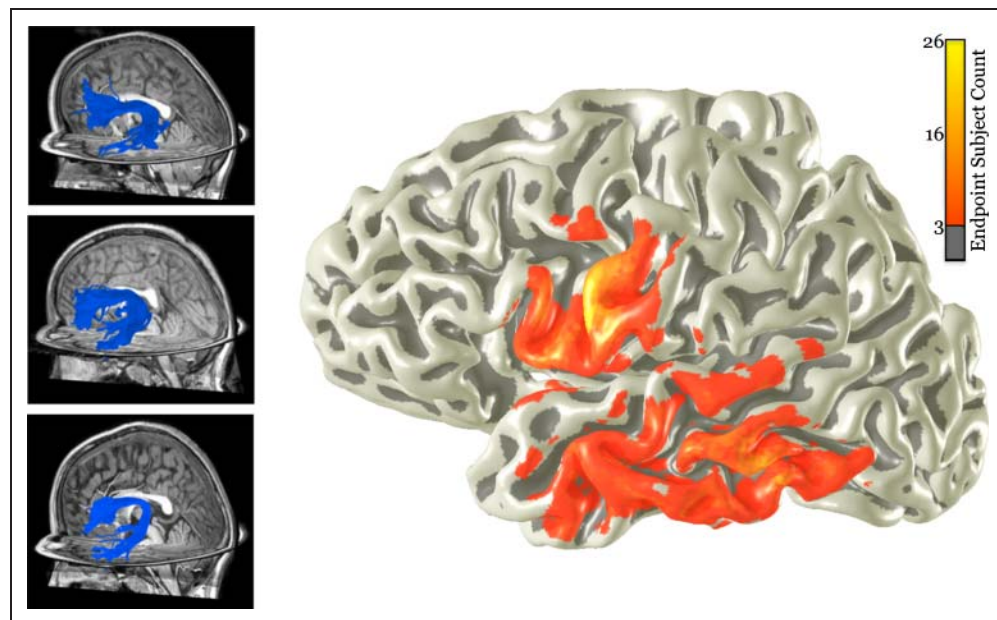
between subjects. Many subjects have AF branching fibers across the superior, middle, and inferior temporal gyri, whereas others have compact AF terminations in the posterior temporal lobe. The arcuate is a complex tract that contains contributions from a wide array of cortical regions, and the microstructure properties estimated within the core of the arcuate probably contain contributions from axons originating in a large part of cortex.

### AF Diffusion Measurements Correlate with Phonological Awareness

Averaged across the entire left AF, FA is negatively correlated with phonological awareness ( $r = -.33, p = .01$ ; Figure 3A). This correlation arises because children with better phonological abilities have greater RD ( $r = .30, p = .02$ ) than children with poor phonological abilities (Figure 3B), but AD ( $r = -.02, p = .88$ ) is independent of phonological ability (Figure 3C). The magnitude of the correlation is the same for men and women, and it is also the same for younger (7–9 years) and older children (10–11 years). Furthermore, the correlation remains significant after covarying for age. The principal correlation we observe is between RD and reading skills, and we examine the finding in a number of different ways.

First, we considered whether alternative methods of identifying the AF might change the result. We identified the AF using an automated procedure to remove any possible experimenter biases (see Methods). The AF identified using this method was similar. The FA ( $r = .85$ ), RD ( $r = .95$ ), and AD values ( $r = .82$ ) estimated using the two segmentation methods were highly correlated but not identical. Even so, the FA and RD of the automatically segmented tracts was significantly correlated with phonological awareness scores ( $r = .3, p = .03$ ). Hence, the

**Figure 2.** Cortical endpoints of the left AF in 55 children. Manually identified left AF fiber groups for three representative children are shown on the left. The frontal lobe endpoints are generally focused in the precentral gyrus and Brodmann's area 44 of the inferior frontal gyrus, whereas the temporal lobe endpoints are spread over significantly more surface area. The heat map on the right shows the number of subjects with left AF endpoints at each region of the cortex. Endpoints for each subject were registered onto the cortical surface of an individual child.



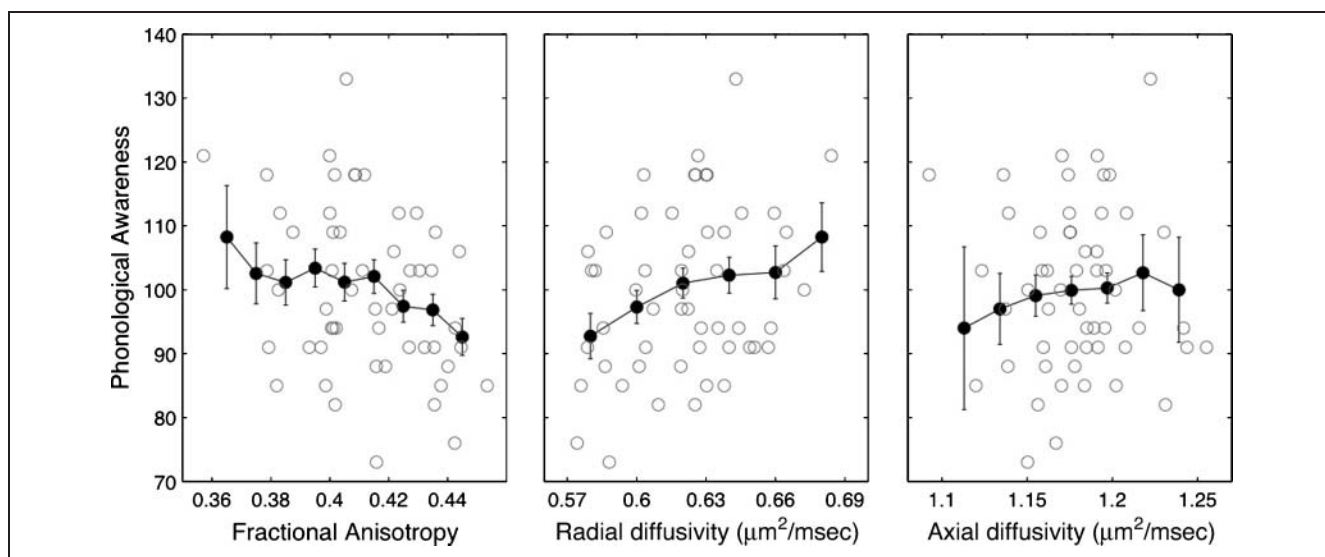


**Figure 3.** Microstructural properties of the left AF correlate with phonological awareness standard scores. FA, RD, and AD are plotted against age-standardized measures of phonological awareness. Solid black circles show mean phonological awareness scores ( $\pm 1 SE$ ) at evenly spaced intervals of FA, RD, and AD. FA is significantly negatively correlated ( $r = -.33$ ), RD is significantly positively correlated ( $r = .30$ ), and AD is not correlated with phonological awareness.

correlation does not depend on the specific tract identification method.

Second, we considered whether the correlation with performance is behaviorally specific to phonological awareness. We found that none of the other behavioral measures were significantly correlated with FA in the left AF. Furthermore, the FA values in left AF remained a significant predictor of phonological awareness after controlling for the effect of general intelligence.

Third, we asked whether this correlation was anatomically specific to the left AF. We found that diffusion properties of three control tracts—the right AF, left corona radiata, and left fronto-parietal SLF—were not significantly correlated with either phonological awareness, phonological memory, or reading. We particularly concentrated on the question of whether the correlation between phonological awareness and FA differed between right and left AF. The mean left AF correlation was  $-0.33$ , whereas the right AF correlation was  $0.05$ . Using bootstrap methods, we estimate the 95% confidence interval on the correlation difference to be between  $0.04$  and  $0.56$ , confirming a reliable difference between them.

Hence, among the measured tracts, only the left AF is correlated with phonological awareness, and among the measured behaviors, the left AF is only correlated with phonological awareness. The anatomical and behavioral specificity of these findings ensures that these results do not reflect general developmental processes.

### Within-subject Diffusivity Varies Significantly along the Length of the AF

By plotting FA along the trajectory of the AF fiber group core (see Supplementary Methods), we found that FA var-

ies considerably at different positions along the tract (Figure 4A). Although some of the FA variation may be intrinsic to the tract, the rest is probably explained by the geometry of the tract and neighboring tracts (i.e., partial voluming with crossing fibers). There is a particularly strong decrease in FA in the region where the arcuate bends most sharply (its principal arc). In this region of high curvature, there are nearby tracts with differing orientations that pass through the same voxels as the arcuate (Figure 4B). The dip in FA in this region reflects both the high curvature and partial voluming with other paths. Along the part of the arcuate that is medial to the central sulcus, fronto-parietal SLF fibers pass closely and follow a parallel trajectory (Figure 4C). Hence, FA in this region is relatively high.

Diffusion measurements averaged along the entire tract confound microstructural differences within the tract of interest with microstructural properties and orientation differences of adjacent tracts. We, therefore, undertook additional measures to assess whether the AF correlation with phonological skills might be explained by the geometry of the AF or the properties of other nearby fibers. To exclude confounds from the pathways near the arc, we selected a compact segment of the AF that is anterior to the arc but posterior to the location in which the arcuate branches into cortex. We identified this region in individual subjects using a three-step protocol. First, we examined the location of the FA dip within each subject's brain and determined that the FA dip colocalizes with the principal arc at an anatomically equivalent location near the temporal-parietal junction. However, the position of this dip is not perfectly aligned across subjects (Figure 5A). In the second step, we coregistered the dip in FA across subjects (Figure 5B). Third, we identified a region anterior to

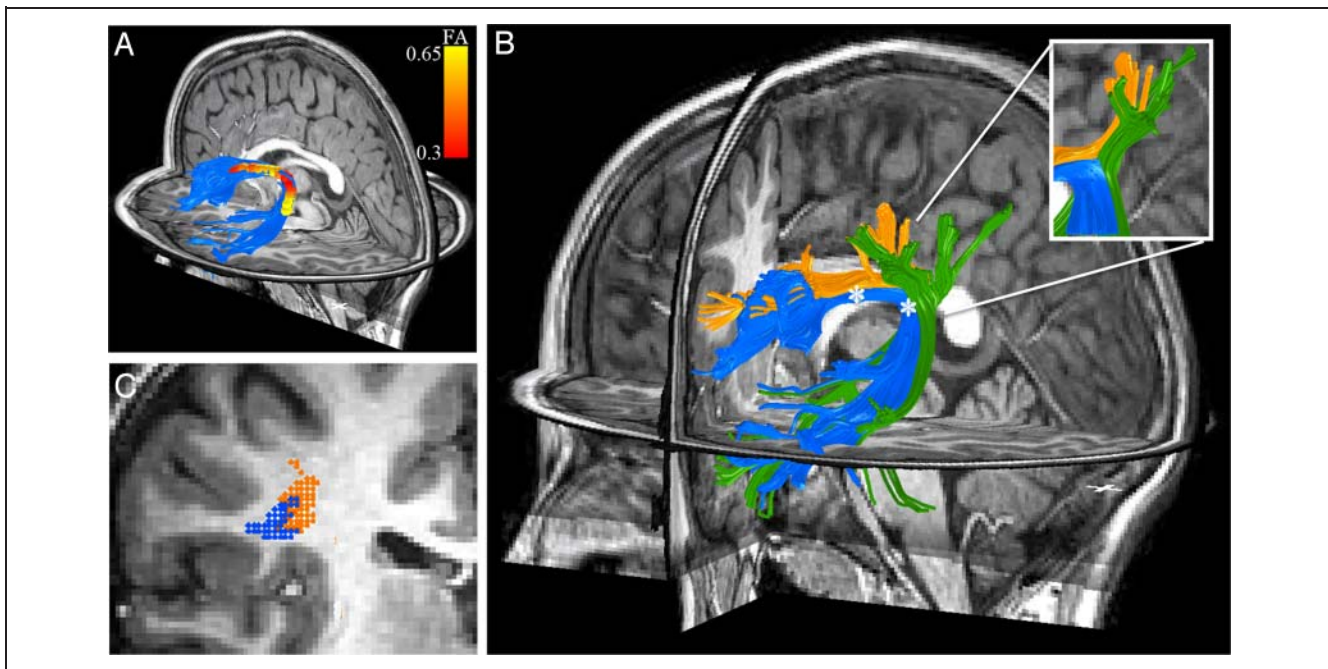


**Figure 4.** FA varies along the trajectory of the AF because of crossing fibers and tract curvature. FA was calculated at 30 nodes along a core section of the AF (A). The 30 nodes for the subject that was most similar to the group mean are displayed as small, overlapping spheres and color-coded red to yellow based on the FA values in that region of the AF (scale bar at the right). Each subject showed a decrease in FA in the arcing region of the tract and an increase in FA in an anterior region of the tract medial to the central sulcus and before the location where fibers branch toward their cortical destinations. (B) Fibers were tracked from 3-mm spheres centered around the node of the highest FA and the node of the lowest FA (asterisks). The AF is shown in blue, non-AF fibers tracked from the high-FA node are shown in orange, and non-AF fibers tracked from the low-FA node are shown in green. The low-FA node contains a mix of AF fibers and fibers that turn laterally and continue to the lateral parietal lobe. The high-FA node contains AF fibers and coherently oriented fibers of the SLF that are destined for the inferior frontal cortex. (C) A coronal slice through the high-FA node shows that, in this region, some voxels along the border of the AF and the SLF are partial volumed between the two tracts; however, a majority (66%) of AF-containing voxels do not contain any SLF fibers.

the principal arc, wherein FA is uncontaminated by fibers traveling in a different direction (Figure 5B, gray-shaded region). Specifically, this region was chosen as the 1-cm portion of the tract with the highest FA.

We reassessed the correlation between FA and phonological awareness on this segment of the AF. This high-FA region contains mainly arcuate fibers; however, some voxels also contain SLF fibers (Figure 4C). This potential

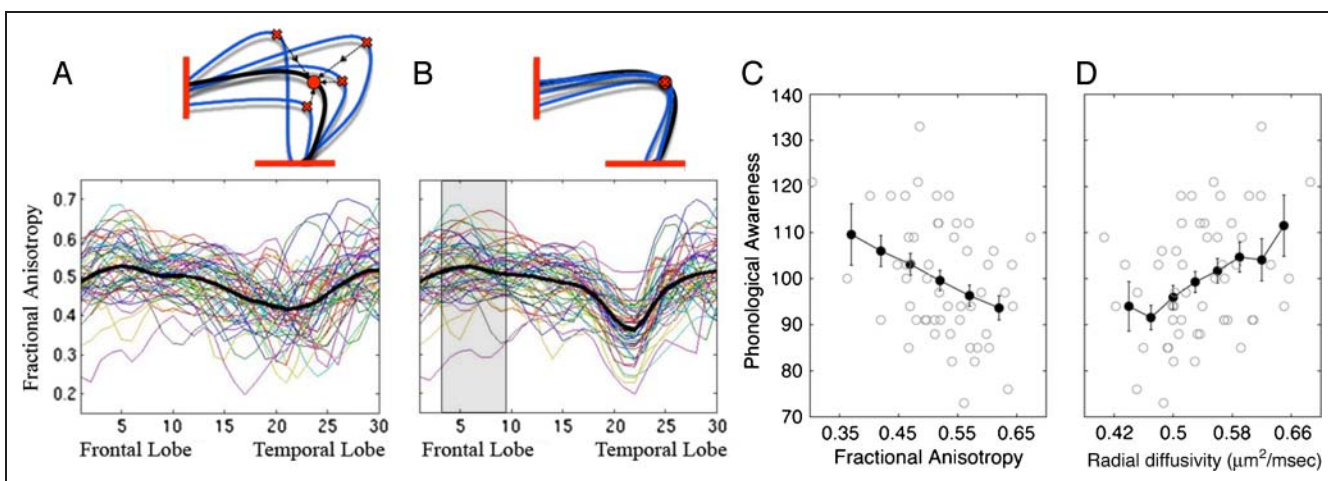


**Figure 5.** Phonological awareness is correlated with AF microstructure in the core region of the AF after individual tracts are aligned. (A) The curved portion of the AF where crossing fibers cause decreased FA is not in register across subjects. (B) Aligning AF trajectories minimizes the confounds of crossing fiber tracts and allows for comparison of microstructural properties in anatomically equivalent regions of the tract across subjects. (C) In a 1-cm region of the tract anterior to the curved portion and posterior to the region where fibers branch toward cortex, FA is significantly negatively correlated with phonological awareness ( $r = -.36$ ). (D) This correlation is driven by a positive correlation between RD and phonological awareness ( $r = .35$ ).

confound was minimized by calculating FA as a weighted average of voxels in this region of the tract where a voxel's weight depends on its distance from the core of the AF. Voxels farther from the core of the tract, which are more likely to be partial volumed with the SLF, contribute less to the measurement (see Supplementary Methods).

Restricted to this region, the correlation between phonological awareness and FA values in the left AF remains significant and is slightly larger ( $r = -.36, p < .01$ ; Figure 5C). Again, this change in FA is because of an increase in RD (Figure 5D).

We had earlier shown that FA on the fronto-parietal SLF, as a whole, did not correlate with phonological awareness. We further examined whether the correlation might be present in measurements restricted only to that portion of the SLF adjacent to the 1-cm portion of the isolated AF. These voxels immediately adjacent to the AF were not significantly correlated with phonological awareness ( $r = -.18, p = .19$ ), confirming the specificity of this effect to the AF.

### AF Volume Laterality

Deterministic tractography identified the left AF in 53 subjects and the right AF in 34 subjects (total  $n = 55$ ). The inability to identify the right AF in 21 subjects using deterministic methods may suggest that the right AF is missing in many brains (Lebel & Beaulieu, 2009; Catani et al., 2007). It is also possible that the right AF is not found because of limitations in deterministic methods that make the right arcuate more problematic for tracking than the left.

Using probabilistic tractography (Sherbondy et al., 2008), we identified a right AF in every subject (Figure 6A). Hence,

the often-reported absence of a right AF reflects limitations of the deterministic algorithm. We compared the probabilistic estimates of the right AF in subjects with and without a deterministic right AF (we term these groups as  $-RAF$  and  $+RAF$ ). There were no qualitative differences in the location, trajectory, or shape of the right AF between the  $-RAF$  and  $+RAF$  groups (Figure 6B). There are differences, however, in the diffusion properties. When we coregister the probabilistic right arcuate tracts (Figure 5B) and measure FA along the trajectory, there is a significant FA reduction in  $-RAF$  subjects compared with  $+RAF$  subjects (Figure 6C). This FA reduction includes the principal arc, where neighboring tracts cross the arcuate.

The reduced FA in the principal arc of the right AF could explain the inability of deterministic methods to identify the tract. Lower FA, as in more spherical tensors, suggests that the PDD in the right arcing region is less reliably measured and likely to estimate an incorrect path direction. Using statistical methods designed to compare PDD estimates between groups of subjects (Schwartzman, Dougherty, & Taylor, 2005), we found that the PDD distributions in the arcing location differ significantly between  $+RAF$  and  $-RAF$  subjects. In subjects where deterministic methods fail to find a right AF, the PDD is relatively lateral–medial; in the subjects where a right AF is found, the PDD is more anterior–posterior.

This suggests that the SLF fibers passing through this region of the AF, destined for the lateral parietal lobe, have a relatively larger effect in the right than the left. This biases the right PDD estimate to align with the SLF rather than the AF. This effect could reflect the volume asymmetry of the AF: A relatively smaller right AF is more easily

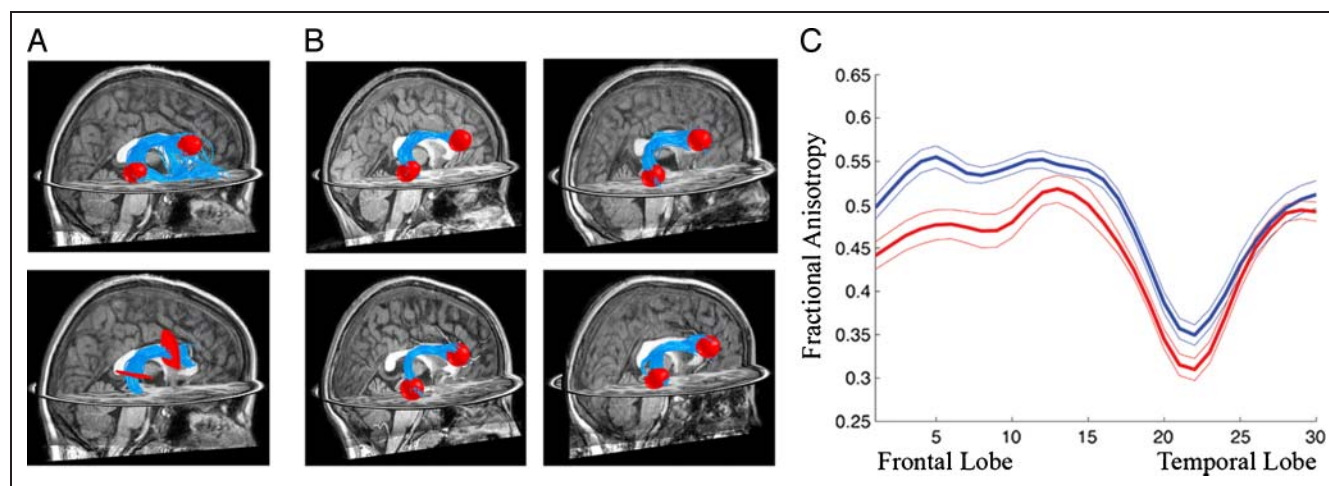


**Figure 6.** Probabilistic tractography identifies the right AF in every subject. (A) The top scored 1000 fibers connecting an ROI in the posterior temporal lobe to an ROI in the inferior frontal lobe (top) are intersected with the waypoint ROIs typically used to define the arcuate (bottom) for a subject who had no identifiable right arcuate with deterministic tractography (STT). (B) A montage of right AF fiber groups tracked with a probabilistic algorithm for two subjects who appeared to be missing the right AF based on STT (top) and two subjects who had right AFs identified with STT (bottom). The AF fiber groups have the same shape and relative position for the two groups of subjects. (C) Comparison of FA along the right AF in two groups of subjects. One group of subjects (blue) had an identifiable AF using deterministic tractography. In the second group of subjects (red), deterministic methods could not identify the right arcuate (although probabilistic methods could). Tracts are aligned with the method shown in Figure 5, and FA is plotted at each node ( $\pm 1 SE$ ).

lost among the branching fibers of the larger frontoparietal SLF.

The small size of the right AF does not imply enhanced left lateralization:  $-RAF$  subjects also tend to have smaller left arcuate volumes ( $-RAF$  subjects:  $M = 19.1 \text{ cm}^3$ ,  $SD = 16.1 \text{ cm}^3$ ;  $+RAF$  subjects:  $M = 30.0 \text{ cm}^3$ ,  $SD = 14.75 \text{ cm}^3$ ;  $t(53) = 2.2$ ,  $p < .05$ ). We suspect that the failure to find the right AF is because of method limitations in finding small pathways that abut larger tracts (in this case, the SLF). The inability to estimate a right arcuate with deterministic methods does not imply a missing or even an extremely lateralized AF but instead reflects relative partial voluming effects of crossing fibers in this region of the brain.

### AF Laterality and Behavior

The deterministic fibers were used to compare the current data with prior reports of left–right volume laterality. We used two laterality measures: (a) a conventional laterality index ( $L$ ) and (b) a measure of the volume difference between left and right arcuates in units of cubic millimeters.

The (unsigned) laterality index  $L$  is defined as

$$L = \frac{|l - r|}{|l + r|}$$

where  $l$  and  $r$  measure the volume of the left and right arcuates. We estimated arcuate laterality based on the automatically segmented tracts.

We use the absolute volume difference to supplement the laterality index because  $L$  is a poor measure in  $-RAF$  participants. For example, consider a subject where we can find only one left AF fiber and we can find no right AF. This subject has the same  $L$  as one with 1000 left AF fibers and none on the right. For this reason, only  $L < 1$  should be considered. We computed the laterality index in the subjects ( $n = 32$ ) with both right and left AF estimates, excluding  $-RAF$  subjects ( $n = 21$ ). The  $-RAF$  and  $+RAF$  participants did not differ in terms of phonological memory ( $t(53) = 0.71$ ,  $p = .50$ ), basic reading skills ( $t(53) = 0.33$ ,  $p = .74$ ), or phonological awareness ( $t(53) = 0.67$ ,  $p = .50$ ).

Five of the subjects with bilateral AFs were right lateralized. Left and right lateralized subjects did not differ on any of the targeted behavioral measures (phonological working memory:  $t(30) = -0.34$ ,  $p = .73$ ; basic reading skills:  $t(30) = 0.05$ ,  $p = .96$ ; phonological awareness:  $t(30) = -0.35$ ,  $p = .72$ ). The data were combined into a group based on the absolute value of laterality to examine the effects of asymmetry irrespective of hemispheric dominance. Figure 7A shows laterality plotted against phonological memory for girls (left) and boys (right). Phonological memory is negatively correlated with laterality for girls ( $r = -.55$ ,  $p = .02$ ,  $n = 18$ ), but not for boys ( $r = -.14$ ,  $p = .63$ ,  $n = 14$ ). This result was independent of

brain volume: The correlation was unaffected when either brain volume or white matter volume was included as a covariate. Furthermore, the correlation was specific to AF laterality and did not represent differences in total cerebral white matter volume between the left and right hemispheres.

To study hemispheric asymmetries for the entire sample, including  $-RAF$  subjects, we calculated the absolute volume difference ( $\text{cm}^3$ ) between the left and right AFs. Figure 7B shows arcuate volume differences plotted against phonological memory for the entire subject population. Phonological memory is negatively correlated with volume differences for girls ( $r = -.45$ ,  $p = .01$ ,  $n = 29$ ), but not for boys ( $r = -.05$ ,  $p = .79$ ,  $n = 24$ ).

Laterality is also negatively correlated with basic reading for girls ( $r = -.53$ ,  $p = .03$ ), but not boys ( $r = .34$ ,  $p = .24$ ). To confirm that these results do not depend on the specific method used to estimate tract volume, we also correlated the phonological memory and basic reading measures with laterality measured using the number of estimated AF streamlines rather than volume. The correlations are the same for laterality measured using fiber count and volume (Supplementary Figure 3).

Phonological awareness is not significantly correlated with laterality. Neither left nor right AF volume correlates with these behavioral measures.

### Combining Brain Measures to Predict Reading Skills

We used multivariate regression to see whether FA in the left arcuate ( $F$ ) and lateralization of the arcuate ( $L$ ) independently contribute to predicting the three behavioral measures ( $B$ ): phonological awareness, phonological memory, and basic reading skills. The model can be summarized as

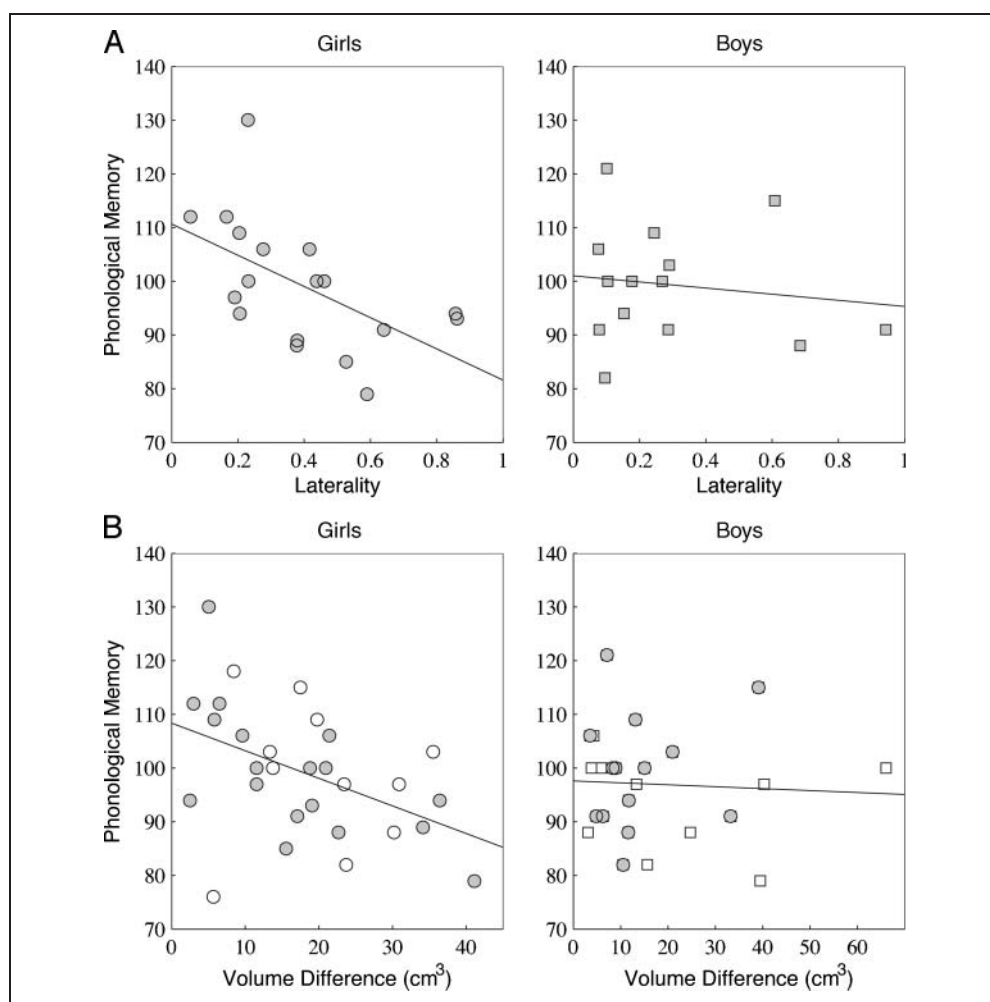
$$B = \omega_1 F + \omega_2 L + \eta$$

This analysis provided new information only with respect to phonological memory. Combining left arcuate FA and volume lateralization of the arcuate increased the variance explained in phonological memory to 35% compared with 15% contributed by lateralization alone. In contrast, when predicting phonological awareness, adding a second variable (lateralization) did not increase the variance explained beyond that of FA alone. Neither FA nor the arcuate lateralization index was a good predictor of basic reading.

### DISCUSSION

The hypothesis that the AF is a critical language pathway is based on a century of clinical observations (Catani & Mesulam, 2008; Catani & Ffytche, 2005; Geschwind, 1965a, 1965b, 1970; Lichtheim, 1885; Wernicke, 1874). Neurological support

**Figure 7.** Scatter plots and regression lines show the relationship between laterality estimates (A) and age standardized phonological memory scores for women ( $r = -.55$ ) and men ( $r = -.14$ ). Women with less lateralized tracts had greater phonological memory scores. The absolute volume difference between left and right hemisphere tracts shows the same correlation with phonological memory (B). Unfilled shapes represent subjects without an identifiable right arcuate using deterministic tracking (-RAF), and filled shapes represent subjects with right and left arcuates (+RAF).



for this hypothesis is based on measures of verbal repetition deficits in subjects with temporal–parietal white matter lesions (Damasio & Damasio, 1980) and deficits in the ability to reactivate phonological working memory representations in such patients (Baldo, Klostermann, & Dronkers, 2008; Friedmann & Gvion, 2003).

Modern neuroimaging supports the role of the AF in language primarily based on cortical terminations (Glasser & Rilling, 2008; Catani et al., 2005) and left lateralization (Lebel & Beaulieu, 2009; Catani et al., 2007; Vernooij et al., 2007) of the pathway. On the basis of the cortical terminations, a number of different hypotheses about the specific language signals carried by the AF have been proposed. These hypotheses span verbal repetition (Ellmore, Beauchamp, O’Neill, Dreyer, & Tandon, 2009; Catani et al., 2005), syntax (Friederici, 2009), and verbalizing semantic knowledge (Rilling et al., 2008).

However, a role for the AF in language is not universally accepted. For example, Schmahmann and Pandya (2006) challenge the language hypothesis, and other authors have proposed new hypotheses about the structure and information carried in the anterior portions of the human AF (Frey, Campbell, Pike, & Petrides, 2008). Using data from macaque anatomy, Schmahmann and Pandya argue

that the AF serves sound localization “but is not related to language per se” (page 408). There is a further debate about the pathways carrying the signals necessary for reading, with some groups suggesting the AF is essential for skilled reading and others suggesting it is not (summarized in Ben-Shachar et al., 2007).

The work presented here is the first to analyze the functional significance of the left AF by measuring language performance and pathway microstructure in individual participants. The principal finding is that pathway microstructure of the left AF correlates with children’s phonological awareness, a skill that is a crucial component of skilled reading (Wagner & Torgesen, 1987). A second finding is that combining estimates of left arcuate microstructure and laterality predicts 35% of the variance in children’s phonological memory performance. These findings support the clinical neurologists’ view that there is a critical role of the AF in language and reading.

### AF Measurements in Individual Brains Correlate with Phonological Skills

The analyses in this article are based on tracking specific fiber groups in individual subjects. We use this approach

because the principal alternative, whole-brain voxel-based analyses, requires coregistering DTI data across subjects. Such methods lack the necessary precision, particularly in the case of the arcuate. For example, Hua et al. (2008) coregistered 28 brains to create a fiber tract template. No voxel in the atlas identified as representing the AF contained AF fibers from more than 20 subjects, and the majority of voxels in the atlas contained significantly fewer subjects (10–14).

A further difficulty with whole-brain analysis is described by Schwartzman et al. (2005), who show that left hemisphere white matter tracts differ in location for good versus poor readers. If the positions of major white matter structures differ between two groups, say good and poor readers, the statistical differences in temporo-parietal diffusion measured by whole-brain group methods may reflect gross anatomical position difference rather than tract microstructure differences (Ben-Shachar et al., 2007).

Recent neurosurgical applications of tractography support the view that tracts relevant to language, including the AF, can be reliably identified in individual subjects (Ellmore et al., 2009). Here, we show that, in the case of the arcuate, identifying the tract in individuals is not enough, because there is extreme variability in FA values along the tract, and the individual FA profiles do not align well. We developed methods to align FA profiles across individuals based on regional variation in tract geometry and calculate diffusion properties at comparable positions along the tract. These methods enhance the power of neurobehavioral correlation analyses within a tract.

### Related Analyses of White Matter Microstructure and Reading

Early group comparisons of good and poor adult readers identified an FA difference in “arcuate-like” voxels (Klingberg et al., 2000). However, further replications of this effect coupled with tracking methods localized correlations between reading and white matter microstructure to the corona radiata (Ben-Shachar et al., 2007; Niogi & McCandliss, 2006; Beaulieu et al., 2005; Deutsch et al., 2005). Furthermore, a recent study that used whole-brain analysis to examine the effects of reading intervention on white matter found increased FA in the centrum semiovale, a nearby region that may contain the same fibers as the anterior corona radiata (Keller & Just, 2009). This is a surprising assignment of function to the corona radiata, which Beaulieu et al. (2005) explained by proposing that the correlation reflected indirect effects of the neighboring AF/SLF.

Niogi and McCandliss (2006) examined whether the corona radiata might have been misidentified in the whole-brain analysis. They undertook an analysis in individual subjects of a single slice containing two ROIs: the corona radiata and a region with a mixture of SLF and AF fibers. They found a correlation between reading and FA in the corona radiata, but not in an ROI, which includes a mixture of fibers from the SLF and the AF.

We did not find a correlation between corona radiata FA and reading skills. The discrepancy between the results of Niogi and McCandliss (2006) and our results is likely because of different methods used for defining ROIs; we measured the whole tract, whereas Niogi and McCandliss selected voxels from a single axial slice along the length of the corona radiata. Given that diffusion properties vary along the trajectory of a tract because of crossing fibers and partial voluming with neighboring structures, we expect that the precise location of the ROI along the length of the corona radiata influences the results.

An earlier analysis of callosal projections in this same cohort of children (Dougherty et al., 2007), as well as two independent replications (Odegard, Farris, Ring, McColl, & Black, 2009; Frye et al., 2008), identified a positive correlation between RD in callosal fibers that project to the temporal lobe and phonological awareness skills. These callosal fibers may terminate in regions of temporal cortex that also contain terminations from AF fibers. Neurons located in the posterior temporal cortex are crucial for the representation of phonological information (Damasio & Damasio, 1980; Wernicke, 1874) and diffusion properties of axon bundles projecting to and from this region may be sensitive biomarkers for reading efficiency.

### Which Functional Signals Are Carried by the AF?

Phonological awareness is the manipulation, decomposition, and synthesis of phonemes and syllables (Wagner et al., 1999; Wagner & Torgesen, 1987). It is likely that phonological awareness signals require communication in both the anterior and posterior directions within the AF fibers. This assumption is supported by functional MRI responses. The AF projects to posterior inferior frontal gyrus (IFG) and ventral premotor cortex (Figure 2). Both regions are consistently responsive in fMRI studies of rhyming and other phonological manipulations (Ben-Shalom & Poeppel, 2008; Poldrack et al., 2001). Moreover, a recent study found that responses in both ventral premotor and posterior temporal regions adapt for the presentation of compressed speech, providing support for the coordinated involvement of these regions in mapping phonological to articulatory codes (Adank & Devlin, 2010). Given the crucial role of phonological awareness for the acquisition of decoding skills in reading, this interpretation of our findings suggests that proper development of the arcuate fibers is essential for healthy reading development, but their contribution to reading is mediated through phonology. This interpretation is in line with a recent case report of a child who developed severe dyslexia after damage to the AF at age of 5 (Rauschecker et al., 2009).

### A Revised Perspective on the Lateralization of the AF

A series of DTI studies report that the AF is left lateralized (Lebel & Beaulieu, 2009; Catani et al., 2007; Eluvathingal,

Hasan, Kramer, Fletcher, & Ewing-Cobbs, 2007; Vernooij et al., 2007; but see Wahl et al., 2010). Specifically, these authors were able to identify the left but not the right arcuate in many subjects. Three separate analyses in this article suggest that the inability to identify the right AF is explained by limitations in DTI fiber-tracking methodologies rather than the absence of the pathway.

First, a probabilistic tracking algorithm succeeds at finding a plausible right AF in every subject. Second, the FA and PDD characteristics of the diffusion data explain why deterministic algorithms may fail to identify a right AF (Figure 6). In the presence of noise, reduced FA makes it more likely for deterministic algorithms to follow the wrong direction. Third, the reduced size of the AF (bilaterally) makes the partial voluming of the neighboring SLF (Figure 4B) more significant and changes the PDD in the right arcing region. Hence, we suspect that the right arcuate is smaller than the left but that the right AF exists in all healthy subjects.

Computational methods that account for the properties of all local pathways should provide more accurate estimates of AF microstructure along the trajectory of the pathway, as well as better estimates of the AF volume (Sherbondy et al., 2009, 2010).

### Behavior and AF Lateralization

There are inconsistent reports about the association between AF lateralization and language abilities in healthy subjects. Lebel and Beaulieu (2009) found a positive correlation between AF lateralization and phonological skills measured by the NEPSY and vocabulary measured by the Peabody Picture Vocabulary Test. However, Catani et al. (2007) found a negative correlation between AF lateralization and verbal recall. We find that lateralization is negatively associated with phonological memory and basic reading for women, but not men (Figure 7).

Aphasia research shows that less lateralized subjects recover better from unilateral lesions because the contralateral hemisphere is able to play a compensatory role (Pizzamiglio, Mammucari, & Razzano, 1985). Our data show that a more bilateral distribution of AF fibers is also beneficial for phonological memory in healthy female children.

Although both phonological working memory and reading rely more heavily on the left hemisphere, these functions recruit right hemisphere homologues as well. It is possible that highly lateralized tracts inhibit the recruitment of contralateral regions during conditions of high cognitive demands. A study of language lateralization in epileptic children found that bilateral activation is associated with better verbal working memory skills, particularly for women, suggesting they are better able to capitalize on compensatory processes in the right hemisphere than are men (Everts et al., 2009). Our findings provide independent support for this hypothesis. This hypothesis should be further investigated with combined

functional and structural imaging methods within the same group of children.

### Interpreting Microstructural Correlations in the Context of Development

Multiple biological structures contribute to the measured diffusion signal. Differences in FA or diffusivity can arise because of microstructural properties of a single tract or they can arise because of different amounts of partial voluming from multiple tracts. In general, diffusivity varies as a function of geometric properties (fiber direction coherence) and the packing density of axons (Stikov et al., 2011; Beaulieu, 2002). Differential packing densities are influenced by a variety of factors including axon caliber, thickness of the myelin sheath, and active developmental processes such as axon pruning, which attenuates the number of axons present in a voxel. In regions of coherent axonal orientation, FA is proportional to the amount of space in a voxel occupied by axons, also called the fiber volume fraction, and is relatively insensitive to the biological properties of those axons.

The functional segregation of brain regions is associated with the pruning of irrelevant connections and the strengthening of pertinent ones through increases in axon caliber and myelin thickness (reviewed in Stiles, 2008; see also LaMantia & Rakic, 1990, 1994). Differences in FA could reflect experience-dependent pruning of axons within the AF fiber bundle, as the pruning of axons would lead to decreased fiber volume fraction.

Another plausible explanation is that decreased FA reflects greater branching of AF axons. We have shown that the temporal lobe endpoints of the AF vary considerably across subjects, hence the relative orientation of axons in the core of the fascicle is also likely to vary. At the microstructural scale measured by diffusion, incoherently oriented axons with highly variable cortical destinations would decrease FA and increase RD.

There are quantitative imaging methods that may be able to provide further clarity about the underlying microstructural changes. The ability to estimate myelin water fraction (MacKay et al., 1994) or bound pool fractions (Stikov et al., 2011; Yarnykh & Yuan, 2004) may provide better information about the local structure that rule out certain classes of explanations.

### Limitations and Future Directions

Developmental structure–function correlations can be suspect for confounding general maturational trends. To rule out such a confound, we demonstrate behavioral and anatomical specificity of the correlation. The correlation between the AF microstructure and behavior is specific to phonological awareness. Furthermore, the correlation is specific to the left AF; neither its right hemisphere homologue nor neighboring tracts in the left hemisphere showed a relationship with phonological or reading skills.

This demonstrates that the effect is not a general maturational process.

The evidence supports the role of the AF in phonological processing of aural information during speech perception and visual information during reading. Longitudinal data on these children can be used to assess how development of the AF influences maturation of language and reading skills.

## Acknowledgments

This work was supported by NIH grant EY015000 to Brian A. Wandell, NSF Graduate Research Fellowship to Jason D. Yeatman, and Marie Curie International Reintegration grant 231029 to Michal Ben-Shachar.

Reprint requests should be sent to Jason D. Yeatman, Wandell Laboratory, Jordan Hall, Building 420, Stanford University, Stanford, CA 94305, or via e-mail: jyeatman@stanford.edu or Michal Ben-Shachar, Gonda Brain Research Center, Bar Ilan University, Ramat Gan 52900, Israel, or via e-mail: michalb@mail.biu.ac.il.

## REFERENCES

- Adank, P., & Devlin, J. T. (2010). On-line plasticity in spoken sentence comprehension: Adapting to time-compressed speech. *Neuroimage*, *49*, 1124–1132.
- Akers, D. (2006). *CINCH: A cooperatively designed marking interface for 3D pathway selection*. Paper presented at the User Interface Software and Technology (UIST), Montreux, Switzerland.
- Baldo, J. V., Klostermann, E. C., & Dronkers, N. F. (2008). It's either a cook or a baker: Patients with conduction aphasia get the gist but lose the trace. *Brain and Language*, *105*, 134–140.
- Basser, P. J., Pajevic, S., Pierpaoli, C., Duda, J., & Aldroubi, A. (2000). In vivo fiber tractography using DT-MRI data. *Magnetic Resonance in Medicine*, *44*, 625–632.
- Basser, P. J., & Pierpaoli, C. (1996). Microstructural and physiological features of tissues elucidated by quantitative-diffusion-tensor MRI. *Journal of Magnetic Resonance, Series B*, *111*, 209–219.
- Beaulieu, C. (2002). The basis of anisotropic water diffusion in the nervous system—A technical review. *NMR in Biomedicine*, *15*, 435–455.
- Beaulieu, C., Plewes, C., Paulson, L. A., Roy, D., Snook, L., Concha, L., et al. (2005). Imaging brain connectivity in children with diverse reading ability. *Neuroimage*, *25*, 1266–1271.
- Ben-Shachar, M., Dougherty, R. F., Wandell, B. A., Ben-Shachar, M., Dougherty, R. F., & Wandell, B. A. (2007). White matter pathways in reading. *Current Opinion in Neurobiology*, *17*, 258–270.
- Ben-Shalom, D., & Poeppel, D. (2008). Functional anatomic models of language: Assembling the pieces. *Neuroscientist*, *14*, 119–127.
- Bernal, B., & Ardila, A. (2009). The role of the arcuate fasciculus in conduction aphasia. *Brain*, *132*, 2309–2316.
- Catani, M., Allin, M. P., Husain, M., Pugliese, L., Mesulam, M. M., Murray, R. M., et al. (2007). Symmetries in human brain language pathways correlate with verbal recall. *Proceedings of the National Academy of Sciences, U.S.A.*, *104*, 17163–17168.
- Catani, M., & Ffytche, D. H. (2005). The rises and falls of disconnection syndromes. *Brain*, *128*, 2224–2239.
- Catani, M., Jones, D. K., & Ffytche, D. H. (2005). Perisylvian language networks of the human brain. *Annals of Neurology*, *57*, 8–16.
- Catani, M., & Mesulam, M. (2008). The arcuate fasciculus and the disconnection theme in language and aphasia: History and current state. *Cortex*, *44*, 953–961.
- Chang, L. C., Jones, D. K., & Pierpaoli, C. (2005). RESTORE: Robust estimation of tensors by outlier rejection. *Magnetic Resonance in Medicine*, *53*, 1088–1095.
- Damasio, H., & Damasio, A. R. (1980). The anatomical basis of conduction aphasia. *Brain*, *103*, 337–350.
- Deutsch, G. K., Dougherty, R. F., Bammer, R., Siok, W. T., Gabrieli, J. D., & Wandell, B. (2005). Children's reading performance is correlated with white matter structure measured by diffusion tensor imaging. *Cortex*, *41*, 354–363.
- Dougherty, R. F., Ben-Shachar, M., Deutsch, G. K., Hernandez, A., Fox, G. R., & Wandell, B. A. (2007). Temporal-callosal pathway diffusivity predicts phonological skills in children. *Proceedings of the National Academy of Sciences, U.S.A.*, *104*, 8556–8561.
- Ellmore, T. M., Beauchamp, M. S., O'Neill, T. J., Dreyer, S., & Tandon, N. (2009). Relationships between essential cortical language sites and subcortical pathways. *Journal of Neurosurgery*, *111*, 755–766.
- Eluvathingal, T. J., Hasan, K. M., Kramer, L., Fletcher, J. M., & Ewing-Cobbs, L. (2007). Quantitative diffusion tensor tractography of association and projection fibers in normally developing children and adolescents. *Cerebral Cortex*, *17*, 2760–2768.
- Everts, R., Simon Harvey, A., Lillywhite, L., Wrennall, J., Abbott, D. F., Gonzalez, L., et al. (2009). Language lateralization correlates with verbal memory performance in children with focal epilepsy. *Epilepsia*, *51*, 627–638.
- Frey, S., Campbell, J. S., Pike, G. B., & Petrides, M. (2008). Dissociating the human language pathways with high angular resolution diffusion fiber tractography. *Journal of Neuroscience*, *28*, 11435–11444.
- Friederici, A. D. (2009). Pathways to language: Fiber tracts in the human brain. *Trends in Cognitive Sciences*, *13*, 175–181.
- Friedmann, N., & Gvion, A. (2003). Sentence comprehension and working memory limitation in aphasia: A dissociation between semantic-syntactic and phonological reactivation. *Brain and Language*, *86*, 23–39.
- Friston, K. J., & Ashburner, J. (2004). Generative and recognition models for neuroanatomy. *Neuroimage*, *23*, 21–24.
- Frye, R. E., Hasan, K., Xue, L., Strickland, D., Malmberg, B., Liederman, J., et al. (2008). Splenium microstructure is related to two dimensions of reading skill. *NeuroReport*, *19*, 1627–1631.
- Geschwind, N. (1965a). Disconnexion syndromes in animals and man. I. *Brain*, *88*, 237–294.
- Geschwind, N. (1965b). Disconnexion syndromes in animals and man. II. *Brain*, *88*, 585–644.
- Geschwind, N. (1970). The organization of language and the brain. *Science*, *170*, 940–944.
- Glasser, M. F., & Rilling, J. K. (2008). DTI tractography of the human brain's language pathways. *Cerebral Cortex*, *18*, 2471–2482.
- Hickok, G., & Poeppel, D. (2004). Dorsal and ventral streams: A framework for understanding aspects of the functional anatomy of language. *Cognition*, *92*, 67–99.
- Hickok, G., & Poeppel, D. (2007). The cortical organization of speech processing. *Nature Reviews Neuroscience*, *8*, 393–402.
- Hua, K., Zhang, J., Wakana, S., Jiang, H., Li, X., Reich, D. S., et al. (2008). Tract probability maps in stereotaxic

- spaces: Analyses of white matter anatomy and tract-specific quantification. *Neuroimage*, *39*, 336–347.
- Jones, D. K. (2004). The effect of gradient sampling schemes on measures derived from diffusion tensor MRI: A Monte Carlo study. *Magnetic Resonance in Medicine*, *51*, 807–815.
- Keller, T. A., & Just, M. A. (2009). Altering cortical connectivity: Remediation-induced changes in the white matter of poor readers. *Neuron*, *64*, 624–631.
- Klingberg, T., Hedehus, M., Temple, E., Salz, T., Gabrieli, J. D., Moseley, M. E., et al. (2000). Microstructure of temporoparietal white matter as a basis for reading ability: Evidence from diffusion tensor magnetic resonance imaging. *Neuron*, *25*, 493–500.
- LaMantia, A. S., & Rakic, P. (1990). Axon overproduction and elimination in the corpus callosum of the developing rhesus monkey. *Journal of Neuroscience*, *10*, 2156–2175.
- LaMantia, A. S., & Rakic, P. (1994). Axon overproduction and elimination in the anterior commissure of the developing rhesus monkey. *Journal of Comparative Neurology*, *340*, 328–336.
- Lebel, C., & Beaulieu, C. (2009). Lateralization of the arcuate fasciculus from childhood to adulthood and its relation to cognitive abilities in children. *Human Brain Mapping*, *30*, 3563–3573.
- Lenroot, R. K., Gogtay, N., Greenstein, D. K., Wells, E. M., Wallace, G. L., Clasen, L. S., et al. (2007). Sexual dimorphism of brain developmental trajectories during childhood and adolescence. *Neuroimage*, *36*, 1065–1073.
- Lichtheim, L. (1885). On aphasia. *Brain*, *7*, 433–484.
- MacKay, A., Whittall, K., Adler, J., Li, D., Paty, D., & Graeb, D. (1994). In vivo visualization of myelin water in brain by magnetic resonance. *Magnetic Resonance in Medicine*, *31*, 673–677.
- Mori, S., Crain, B. J., Chacko, V. P., & van Zijl, P. C. (1999). Three-dimensional tracking of axonal projections in the brain by magnetic resonance imaging. *Annals of Neurology*, *45*, 265–269.
- Mori, S., Wakana, S., van Zijl, P. C., & Nagae-Poetscher, L. M. (2005). *MRI atlas of human white matter*. Amsterdam: Elsevier.
- Niogi, S. N., & McCandliss, B. D. (2006). Left lateralized white matter microstructure accounts for individual differences in reading ability and disability. *Neuropsychologia*, *44*, 2178–2188.
- Odegard, T. N., Farris, E. A., Ring, J., McColl, R., & Black, J. (2009). Brain connectivity in non-reading impaired children and children diagnosed with developmental dyslexia. *Neuropsychologia*, *47*, 1972–1977.
- Pizzamiglio, L., Mammucari, A., & Razzano, C. (1985). Evidence for sex differences in brain organization in recovery in aphasia. *Brain and Language*, *25*, 213–223.
- Poldrack, R. A., Temple, E., Protopoulos, A., Nagarajan, S., Tallal, P., Merzenich, M., et al. (2001). Relations between the neural bases of dynamic auditory processing and phonological processing: Evidence from fMRI. *Journal of Cognitive Neuroscience*, *13*, 687–697.
- Rauschecker, A. M., Deutsch, G. K., Ben-Shachar, M., Schwartzman, A., Perry, L. M., & Dougherty, R. F. (2009). Reading impairment in a patient with missing arcuate fasciculus. *Neuropsychologia*, *47*, 180–194.
- Rilling, J. K., Glasser, M. F., Preuss, T. M., Ma, X., Zhao, T., Hu, X., et al. (2008). The evolution of the arcuate fasciculus revealed with comparative DTI. *Nature Neuroscience*, *11*, 426–428.
- Rohde, G. K., Barnett, A. S., Basser, P. J., Marengo, S., & Pierpaoli, C. (2004). Comprehensive approach for correction of motion and distortion in diffusion-weighted MRI. *Magnetic Resonance in Medicine*, *51*, 103–114.
- Saur, D., Kreher, B. W., Schnell, S., Kummerer, D., Kellmeyer, P., Vry, M. S., et al. (2008). Ventral and dorsal pathways for language. *Proceedings of the National Academy of Sciences, U.S.A.*, *105*, 18035–18040.
- Schmahmann, J. D., & Pandya, D. N. (2006). *Fiber pathways of the brain*. New York: Oxford University Press.
- Schwartzman, A., Dougherty, R. F., & Taylor, J. E. (2005). Cross-subject comparison of principal diffusion direction maps. *Magnetic Resonance in Medicine*, *53*, 1423–1431.
- Sherbondy, A. J., Dougherty, R. F., Ananthanarayanan, R., Modha, D. S., & Wandell, B. A. (2009). Think global, act local: projectome estimation with BlueMatter. *Medical Image Computing and Computer-Assisted Intervention*, *12*, 861–868.
- Sherbondy, A. J., Dougherty, R. F., Ben-Shachar, M., Napel, S., & Wandell, B. A. (2008). ConTrack: Finding the most likely pathways between brain regions using diffusion tractography. *Journal of Vision*, *8*, Article 15.
- Sherbondy, A. J., Matthew, R., & Alexander, D. C. (2010). MicroTrack: An algorithm for concurrent projectome and microstructure estimation. *Lecture Notes in Computer Science–MICCAI 2010*, *6361*, 183–190.
- Stikov, N., Perry, L. M., Mezer, A., Rykhlevskaia, E., Wandell, B. A., Pauly, J. M., et al. (2011). Bound pool fractions complement diffusion measures to describe white matter micro and macrostructure. *Neuroimage*, *54*, 1112–1121.
- Stiles, J. (2008). *The fundamental of brain development integrating nature and nurture*. Cambridge, MA: Harvard University Press.
- Vernooij, M. W., Smits, M., Wielopolski, P. A., Houston, G. C., Krestin, G. P., & van der Lugt, A. (2007). Fiber density asymmetry of the arcuate fasciculus in relation to functional hemispheric language lateralization in both right- and left-handed healthy subjects: A combined fMRI and DTI study. *Neuroimage*, *35*, 1064–1076.
- Wagner, R., & Torgesen, J. (1987). The nature of phonological processing and its causal role in the acquisition of reading skills. *Psychological Bulletin*, *101*, 192–212.
- Wagner, R., Torgesen, J., & Rashotte, C. A. (1999). *Comprehensive test of phonological processes (CTOPP)*. Austin, TX: Pro-Ed.
- Wahl, M., Li, Y. O., Ng, J., Lahue, S. C., Cooper, S. R., Sherr, E. H., et al. (2010). Microstructural correlations of white matter tracts in the human brain. *Neuroimage*, *51*, 531–541.
- Wernicke, K. (1874). *The aphasia symptom-complex* (Vol. 4). Amsterdam: John Benjamins.
- Woodcock, R. W., McGrew, K. S., & Mather, N. (2001). *Woodcock Johnson III Tests of Achievement*. Itaska, IL: Riverside Publishing.
- Yarnykh, V. L., & Yuan, C. (2004). Cross-relaxation imaging reveals detailed anatomy of white matter fiber tracts in the human brain. *Neuroimage*, *23*, 409–424.